Non-Data Aided Feedforward Cyclostationary Statistics Based Carrier Frequency Offset Estimators for Linear Modulations

Y. Wang[1], E. Serpedin[1], P. Ciblat[2], and P. Loubaton[3]

[1] Dept. of Electrical Engineering, Texas A&M University, College Station, TX 77843, USA

[2] Université Catholique de Louvain, Lab. "Télédétection et Télécommunications", Belgium

[3] Université de Marne-la-Vallée, Lab. "Systèmes de Communication", Marne-la-Vallée , France

Abstract— **This paper proposes to analyze the performance of a family of non-data aided open-loop carrier frequency offset (FO) estimators for a linearly modulated signal transmitted through an unknown flat-fading (possibly frequency-selective) channel. The exact asymptotic (large sample) performance of these estimators is established and analyzed as a function of the received signal sampling frequency, signal-to-noise ratio (SNR), timing delay, and number of samples (N). It is shown that in the presence of timing errors, the performance of the estimators can be improved by oversampling (fractionally sampling) the received signal and by taking into account the entire cyclostationary information that is present in the received sequence.**

I. INTRODUCTION

In mobile wireless communication channels, loss of synchronization may occur due to carrier frequency offset and/or Doppler effects. It appears that non-data aided (or blind) open loop carrier frequency offset estimation schemes that do not require training sequences and necessitate short acquisition time present high potential for synchronization of burst mode transmissions and spectrally efficient modulations.

Non-data aided open-loop carrier frequency offset estimators that exploit the cyclostationary (CS) statistics of the received waveform have been proposed and partially analyzed by many researchers (see e.g., [1]-[7]). The common feature of these algorithms relies on exploiting the CS statistics that are induced either by oversampling of the received analog waveform [5] or by processing the received discrete-time sequence through a nonlinear device [1], [3], [4], [6]. This later category of estimators exploit the second and/or the fourth-order CS statistics of the received sequence and exhibit high convergence rates (asymptotic variance on the order of $O(N^{-3})$, where N stands for the number of samples).

This paper proposes to study in a rigorous and systematic way the exact asymptotic (large sample) performance of these estimators and to propose new algorithms that improve the performance of the existing estimators. Due to space limitations, we will present our study only for real-valued (BPSK and PAM) and general QAM constellations transmitted through flat-fading channels.

II. MODELING ASSUMPTIONS

Suppose that a linearly modulated signal is transmitted through a flat-fading channel. The complex envelope of the received signal is affected by a carrier frequency offset and/or Doppler shift F_e [2] and is given by[1]:

$$r_c(t) = e^{j2\pi F_e t} \sum_l w(l) h_c^{(tr)}(t - lT - \epsilon T) + v_c(t) \ , \quad (1)$$

where $w(l)$'s are the transmitted symbols, $h_c^{(tr)}(t)$ denotes the transmitter's signaling pulse, $v_c(t)$ is the complex-valued additive noise assumed independently distributed with respect to (w.r.t.) the input symbol sequence $w(n)$, T is the symbol period, and ϵ is an unknown timing error. After matched filtering with $h_c^{(rec)}(t)$, the resulting signal is (over)sampled at a period $T_s := T/P$, where the oversampling factor $P \geq 1$ is an integer. The following equivalent discrete-time model can be deduced:

$$x(n) = e^{j2\pi f_e n} \sum_l w(l) h(n - lP) + v(n) \ , \quad (2)$$

where $f_e := F_e T_s$, $x(n) := (r_c(t) \otimes h_c^{(rec)}(t))|_{t=nT_s}$ ($\otimes$ denotes convolution), $v(n) := (v_c(t) \otimes h_c^{(rec)}(t))|_{t=nT_s}$ and $h(n) := (h_c^{(tr)}(t) \otimes h_c^{(rec)}(t))|_{t=nT_s - \epsilon T}$.

In order to simplify the derivation of the asymptotic performance of the FO-estimators, the following assumptions are imposed:

(**AS1**) $w(n)$ is a zero-mean i.i.d. sequence with values drawn from a linearly modulated complex constellation with unit variance, i.e., $\sigma_{2w}^2 := \mathrm{E}|w(n)|^2 = 1$.

(**AS2**) $v_c(t)$ is circularly white normally distributed with zero mean and variance σ_v^2.

(**AS3**) the transmit and receive filters are square-root raised cosine pulses of bandwidth $[-(1+\rho)/2T, (1+\rho)/2T]$, where the parameter ρ represents the roll-off factor ($0 \leq \rho < 1$).

(**AS4**) frequency offset F_e is small enough so that the mismatch of the receive filter due to F_e can be neglected [5]. Generally, the condition $F_e T < 0.1$ is assumed.

III. CARRIER FREQUENCY OFFSET ESTIMATORS

Estimating f_e from $x(n)$ in (2) amounts to retrieving a complex exponential embedded in multiplicative noise $\sum_l w(l)h(n - lP)$ and additive noise $v(n)$ [6]. The underlying idea for estimating the frequency offset is to interpret the received signal higher order statistics as a sum of several constant amplitude harmonics embedded in noise, and to extract the carrier offset from the frequencies of these spectral lines. We will solve this spectral analysis problem by mapping this problem into a CS-statistics framework. It turns out that if the input symbol constellation is real-valued (BPSK, PAM), then it follows that $\mathrm{E}\{w^2(n)\} \neq 0$, and thus the second-order CS statistics of $x(n)$ can be used to recover f_e. Due to their $\pi/2$-rotationally invariant symmetry properties, all QAM constellations satisfy the moment conditions $\mathrm{E}\{w^2(n)\} = \mathrm{E}\{w^3(n)\} = 0$, $\mathrm{E}\{w^4(n)\} \neq 0$, and con-

[1]The subscript $_c$ is used to denote a continuous-time signal.

sequently FO-estimators may be designed based on the the fourth-order CS-statistics of the received sequence.

A. BPSK or PAM Constellations

Since $\mathrm{E}\{w^2(n)\} \neq 0$ for real-valued constellations, the second order unconjugated cyclic correlations of $x(n)$ will be exploited to estimate the carrier frequency offset. First, in the case $P = 1$, the unconjugated time-varying correlation of the output is given by:

$$\widetilde{c}_{2x}(n;\tau):=\mathrm{E}\{x(n)x(n+\tau)\}=e^{j2\pi f_e(2n+\tau)}\sum_l h(l)h(l+\tau).$$

Being almost periodic with respect to n, the generalized Fourier Series (FS) coefficients of $\widetilde{c}_{2x}(n;0)$, termed unconjugated cyclic correlations, are given by (c.f. [2]):

$$\begin{aligned}\widetilde{C}_{2x}(\alpha;0) &:= \lim_{N\to\infty}\frac{1}{N}\sum_{n=0}^{N-1}\widetilde{c}_{2x}(n;0)e^{-j2\pi\alpha n}\\ &= \widetilde{C}_{2x}(\alpha_0;0)\delta(\alpha-\alpha_0),\end{aligned} \tag{3}$$

where $\widetilde{C}_{2x}(\alpha_0;0) := \sum_l h^2(l)$ and $\alpha_0 := 2f_e$. From (3), it follows that $\widetilde{C}_{2x}(\alpha;0)$ consists only one spectral line located at cycle $2f_e$. An estimator of f_e can be obtained by measuring the location of this spectral line:

$$f_e = \frac{1}{2}\left(\arg \max_{\alpha\in(-0.5,\ 0.5)}\left|\widetilde{C}_{2x}(\alpha;0)\right|\right) . \tag{4}$$

In practice, a computationally efficient FFT-based implementation of (4) can be expressed as:

$$\hat{f}_e = \frac{1}{2}\left(\arg \max_{\alpha\in(-0.5,\ 0.5)}\left|\frac{1}{N}\sum_{n=0}^{N-1}x^2(n)e^{-j2\pi\alpha n}\right|\right) . \tag{5}$$

In the case when $P > 1$ (for simplicity, we assume $P \geq 4$), an alternative expression of (3) can be expressed as:

$$\widetilde{C}_{2x}(\alpha;0) = \sum_{k=0}^{P-1}\widetilde{C}_{2x}(k;0)\delta(\alpha-(\frac{k}{P}+\alpha_0)) , \tag{6}$$

where $\widetilde{C}_{2x}(k;0) := (1/P)\sum_n h^2(n)\exp(-j2\pi kn/P)$. Due to (**AS3**), it is easy to check that $\widetilde{C}_{2x}(k;0)$ are nonzero only for cycles $k = 0, \pm 1$. Thus, $\widetilde{C}_{2x}(\alpha;0)$ consists of three spectral lines located at cycles $2f_e{+}k/P,\ k = 0,\ \pm 1$ [6]. It is possible to extract f_e solely from the location information of the spectral line of highest magnitude ($k = 0$) and to obtain again the estimator (5). A different alternative is to extract the frequency offset by exploiting jointly the location information of all the three spectral lines. In this case the following FFT-based FO-estimator is obtained:

$$\hat{f}_e=\frac{1}{2}\left(\arg\max_{|\alpha|<1/(2P)}\sum_{k=-1}^{1}\left|\frac{1}{N}\sum_{n=0}^{N-1}x^2(n)e^{-j2\pi(\alpha+\frac{k}{P})n}\right|\right). \tag{7}$$

The condition $|2f_e| \leq 1/(2P)$ is assumed in order to ensure identifiability of f_e.

It is interesting to remark that the previous estimators have been developed by exploiting the CS-statistics information present in the unconjugated time-varying correlation $\widetilde{c}_{2x}(n;\tau)$, for fixed time lag $\tau = 0$. However, by exploiting the information provided by the correlations $\widetilde{c}_{2x}(n;\tau)$ for all the possible values of τ, one may expect to improve the performance of the estimators that rely solely on $\widetilde{c}_{2x}(n;0)$. Some calculations show that the estimator that exploits all the lags τ and only the information provided by the spectral line of largest magnitude takes the form:

$$\hat{f}_e = \frac{1}{2}\left(\arg \max_{\alpha\in(-0.5,\ 0.5)}\sum_{\tau}\left|\frac{1}{N}\sum_{n=0}^{N-1}x(n)x(n+\tau)e^{-j2\pi\alpha n}\right|\right). \tag{8}$$

In [2], we have established the asymptotic performance of the estimator (8) and shown that its performance improves significantly the performance of estimator (5).

B. QAM Constellations

Define the fourth-order unconjugated time-varying correlation of the received sequence $x(n)$ via: $\widetilde{c}_{4x}(n;\mathbf{0}) := \mathrm{E}\{x^4(n)\}$, with $\mathbf{0} := [0\ 0\ 0]$. For $P = 1$, it turns out that:

$$\widetilde{c}_{4x}(n;\mathbf{0}) = \widetilde{\kappa}e^{j2\pi 4f_e n}\sum_l h^4(l) , \tag{9}$$

with $\widetilde{\kappa} := \mathrm{E}\{w^4(n)\}$. Similarly for $P > 1$, we obtain:

$$\widetilde{c}_{4x}(n;\mathbf{0}) = \widetilde{\kappa}e^{j2\pi 4f_e n}\sum_l h^4(n-lP) . \tag{10}$$

It can be shown that $\widetilde{C}_{4x}(\alpha;\mathbf{0})$, the generalized FS coefficient of $\widetilde{c}_{4x}(n;\mathbf{0})$, consists of a single spectral line located at $4f_e$ (when $P = 1$) and P spectral lines located at the cyclic frequencies $4f_e + k/P,\ k = 0,\ 1, \ldots, P-1$ (when $P > 1$). Similar to (5) and (7), the following FFT-based estimators can be obtained if we only consider the spectral line located at $k = 0$:

$$\hat{f}_e=\frac{1}{4}\left(\arg\max_{\alpha\in(-0.5,\ 0.5)}\left|\frac{1}{N}\sum_{n=0}^{N-1}x^4(n)e^{-j2\pi\alpha n}\right|\right), \tag{11}$$

and when all the spectral lines are taken into account, we obtain for $P > 1$ the following FO-estimator:

$$\hat{f}_e=\frac{1}{4}\left(\arg\max_{|\alpha|<1/(2P)}\sum_{k=0}^{P-1}\left|\frac{1}{N}\sum_{n=0}^{N-1}x^4(n)e^{-j2\pi(\alpha+\frac{k}{P})n}\right|\right). \tag{12}$$

As before, the assumption $|4f_e| \leq 1/(2P)$ is necessary in (11) and (12) to ensure identifiability of f_e.

IV. PERFORMANCE ANALYSIS

In this section, we will establish first the asymptotic performance of the FO-estimator (7) and extend later on this analysis to the estimators (5), (11) and (12). Due to lack of space the asymptotic performance of estimator (8) and its variants (for BPSK/QPSK constellations, $P = 1$ and $P > 1$) will be reported in a future paper. From the definition of unconjugated cyclic correlation and (6), the unconjugated time-varying correlation $\widetilde{c}_{2x}(n;0)$ can be expressed as:

$$\widetilde{c}_{2x}(n;0)=\sum_{k=-1}^{1}\widetilde{C}_{2x}(k;0)e^{j2\pi(\frac{k}{P}+\alpha_0)n}=\sum_{k=-1}^{1}\lambda_k e^{j(\omega_k n+\phi_k)},$$

where: $\lambda_k e^{j\phi_k} := \widetilde{C}_{2x}(k;0)$, and $\omega_k := (2\pi k/P) + 2\pi\alpha_0$. Defining the zero-mean stochastic process $e(n)$ as:

$$e(n):=x^2(n) - \mathrm{E}\{x^2(n)\} = x^2(n)-\sum_{k=-1}^{1}\lambda_k e^{j(\omega_k n+\phi_k)}, \quad (13)$$

it follows that:

$$x^2(n) = \sum_{k=-1}^{1}\lambda_k e^{j(\omega_k n+\phi_k)} + e(n) \ .$$

Thus, $x^2(n)$ can be interpreted as the sum of three constant amplitude harmonics corrupted by the cyclostationary noise $e(n)$ [2], [6]. Consider the nonlinear least-squares estimator (NLS):

$$\hat{\boldsymbol{\theta}} := \arg\min_{\boldsymbol{\theta}} J(\boldsymbol{\theta}) \ , \quad (14)$$

$$J(\boldsymbol{\theta}) := \frac{1}{N}\sum_{n=0}^{N-1}\left|x^2(n) - \sum_{k=-1}^{1}\lambda_k e^{j(\omega_k n+\phi_k)}\right|^2 \ , \quad (15)$$

where $\boldsymbol{\theta} := [\lambda_{-1}\ \phi_{-1}\ \lambda_0\ \phi_0\ \lambda_1\ \phi_1\ \alpha_0]^T$. It can be shown that the FFT-based estimator (7) is asymptotically equivalent to the NLS-estimator (14) (see e.g., [7]). Hence, in order to compute the asymptotic performance of estimator (7), it suffices to establish the asymptotic performance of NLS-estimator (14) [6]. By adopting the lines of proof presented in [7], some lengthy calculations lead to the following expression for the FO-estimator's asymptotic variance:

$$\lim_{N\to\infty} N^3\mathrm{E}\{(\hat{\alpha}_0-\alpha_0)^2\} = 6\sum_{k=0}^{P-1}\sum_{l=0}^{P-1}\lambda_k\lambda_l$$
$$\cdot\ \mathrm{Re}\{e^{j(\phi_k-\phi_l)}S_{2e}(k-l;\omega_k)\}/(\sum_{k=0}^{P-1}\lambda_k^2)^2 \ . \quad (16)$$

As a particular case of (16), the asymptotic variance of estimator (5) can be expressed as:

$$\lim_{N\to\infty} N^3\mathrm{E}\{(\hat{\alpha}_0-\alpha_0)^2\} = \frac{6S_{2e}(0;\omega_0)}{\lambda_0^2} \ , \quad (17)$$

where $S_{2e}(0;\omega_0)$ denotes the cyclic spectrum of $e(n)$. Note that when $P = 1$, $e(n)$ is stationary w.r.t. its autocorrelation function and the cyclic spectrum $S_{2e}(0;\omega_0)$ coincides with the second order stationary spectrum $S_{2e}(\omega_0)$.

It is not difficult to find that the previous derivations also hold for the estimators (11) and (12). Just by replacing (13) with the following expression:

$$e(n) := x^4(n) - \mathrm{E}\{x^4(n)\} = x^4(n) - \sum_{k=0}^{P-1}\lambda_k e^{j(\omega_k n+\phi_k)} \ , \quad (18)$$

with:

$$\lambda_k e^{j\phi_k} := \widetilde{C}_{4x}(k;\mathbf{0}) = \frac{\widetilde{\kappa}}{P}\sum_n h^4(n)e^{-j2\pi kn/P} \ ,$$
$$\omega_k := \frac{2\pi k}{P} + 4\pi\alpha_0 \ ,$$

and by repeating the same calculations as above, the same asymptotic variance expressions (16) and (17) are obtained for estimators (11) and (12).

Evaluation of asymptotic variance (17) requires calculation of cyclic spectrum: $S_{2e}(0,\omega_0)$. In what follows, we will present the closed-form expressions of the stationary/CS spectra $S_{2e}(\omega_0)$ and $S_{2e}(0;\omega_0)$.

A. BPSK or PAM Constellations

Define the second-order conjugated autocorrelations and cyclic correlations of the received sequence $x(n)$ as:

$$c_{2x}(n;\tau) := \mathrm{E}\{x^*(n)x(n+\tau)\}$$
$$= e^{j2\pi f_e\tau}\sum_l h(n-lP)h(n+\tau-lP) + \sigma_v^2 g(\tau),$$
$$C_{2x}(k;\tau)=\frac{e^{j2\pi f_e\tau}}{P}\sum_n h(n)h(n+\tau)e^{-\frac{j2\pi kn}{P}} + \sigma_v^2 g(\tau)\delta(k),$$

where $g(n)$ stands for the raised-cosine pulse shape. The following results hold:

Proposition 1. *The stationary spectrum of* $e(n)$ *(*$P = 1$*) is given by:*

$$S_{2e}(\omega_0)=2\sum_\tau c_{2x}^2(\tau)e^{-j\omega_0\tau}+\kappa_4\sum_\tau\sum_l h^2(l)h^2(l+\tau), \quad (19)$$

where κ_4 *denotes the kurtosis of* $w(n)$.

Proposition 2. *The cyclic spectrum of* $e(n)$ *(*$P > 1$*) is given by:*

$$S_{2e}(0;\omega_0) = 2\sum_\tau\left[2C_{2x}(-1;\tau)C_{2x}(1;\tau) + C_{2x}^2(0;\tau)\right]$$
$$\cdot e^{-j\omega_0\tau} + \kappa_4 P|\widetilde{C}_{2x}(0;0)|^2 \ , \quad (20)$$

B. QPSK or QAM Constellations

As opposed to the real-valued constellations mentioned above, the FO-estimators corresponding to QAM constellations rely on the higher-order statistics of $x(n)$. Define the variables:

$$\sigma_{4w}^2 := \mathrm{E}\{w^{*2}(n)w^2(n)\} \ , \ \sigma_{6w}^2 := \mathrm{E}\{w^{*3}(n)w^3(n)\} \ ,$$
$$\kappa_8 := \mathrm{cum}\{w^*(n), w^*(n), w^*(n), w^*(n), w(n), w(n), w(n), w(n)\} \ ,$$

and the fourth and sixth-order unconjugated autocorrelations/cyclic correlations of $x(n)$ as:

$$c_{4x}(n;0,\tau,\tau) := \mathrm{E}\{x^{*2}(n)x^2(n+\tau)\} ,$$

$$C_{4x}(k;0,\tau,\tau) := \frac{1}{P}\sum_{n=0}^{P-1} c_{4x}(n;0,\tau,\tau)e^{-j2\pi kn/P} ,$$

$$c_{6x}(n;0,0,\tau,\tau,\tau) := \mathrm{E}\{x^{*3}(n)x^3(n+\tau)\} ,$$

$$C_{6x}(k;0,0,\tau,\tau,\tau) := \frac{1}{P}\sum_{n=0}^{P-1} c_{6x}(n;0,0,\tau,\tau,\tau)e^{-j2\pi kn/P}.$$

After some straightforward but lengthy calculations, the following results can be established:

Proposition 3. *The stationary spectrum of* $e(n)$ *(*$P = 1$*) is given by:*

$$\begin{aligned} S_{2e}(\omega_0) = \sum_\tau \Big[&16c_{2x}(\tau)c_{6x}(0,0,\tau,\tau,\tau) + 36c_{4x}^2(0,\tau,\tau) \\ &- 72c_{2x}^2(\tau)c_{4x}(0,\tau,\tau) + 24c_{2x}^4(\tau)]e^{-j\omega_0\tau} \\ &+ \kappa_8\sum_\tau\sum_l h^4(l)h^4(l+\tau) . \end{aligned} \tag{21}$$

Proposition 4. *The cyclic spectrum of* $e(n)$ *(*$P > 1$*) is given by:*

$$\begin{aligned} S_{2e}(0;\omega_0) = &\sum_\tau(16\mathcal{V}_1 + 36\mathcal{V}_2 - 72\mathcal{V}_3 + 24\mathcal{V}_4)e^{-j\omega_0\tau} \\ &+\frac{\kappa_8 P}{\widetilde{\kappa}^2}|\widetilde{C}_{4x}(0;\mathbf{0})|^2 , \end{aligned} \tag{22}$$

where

$$\mathcal{V}_1 := \sum_{k=-1}^{1} C_{2x}(k;\tau)C_{6x}(-k;0,0,\tau,\tau,\tau) ,$$

$$\mathcal{V}_2 := \sum_{k=0}^{P-1} C_{4x}(k;0,\tau,\tau)C_{4x}(P-k;0,\tau,\tau) ,$$

$$\mathcal{V}_3 := \sum_{k=-1}^{1}\sum_{l=-1}^{1}\sum_{\substack{m=0 \\ k+l+m\equiv 0 \bmod P}}^{P-1} C_{2x}(k;\tau)C_{2x}(l;\tau)C_{4x}(m;0,\tau,\tau),$$

$$\mathcal{V}_4 := \sum_{\substack{k_i=-1 \\ \sum_i k_i \equiv 0 \bmod P}}^{1} \prod_{i=0}^{3} C_{2x}(k_i;\tau) .$$

V. SIMULATIONS AND RESULTS

In this section, the experimental mean-square error (mse) results and theoretical asymptotic bounds will be compared. The experimental results are obtained by performing a number of 100 Monte Carlo trials assuming that the transmitted symbols are selected from BPSK/QPSK constellations with $\sigma_w^2 = 1$. The transmit and receive filters are square-root raised cosine filters with roll-off factor $\rho = 0.5$, and the additive noise is generated by passing Gaussian white noise with variance σ_v^2 through the square-root raised cosine filter. The signal-to-noise ratio is defined as: SNR:= $10\log_{10}(\sigma_w^2/\sigma_v^2)$. All the simulations are performed assuming the frequency offset $f_eT = 0.011$. In [2], we have found that the performance of estimator (8) is very close to the performance achieved by the estimator (5) in an ideal case of no ISI-effects (i.e., perfect knowledge of the time delay). The theoretical asymptotic variance of estimator (8) is depicted in Fig. 1 and Fig. 3 by the dash-dot line. In Figures 1–6, the theoretical bounds of estimators (5) and (11) for $P = 1$ and $P = 4$ are represented by the solid line and the solid line with stars, respectively. The experimental results of estimators (5) and (11) for $P = 1$ and $P = 4$ are plotted using dash lines with circles and squares, respectively.

Experiment 1-Performance w.r.t. SNR: Assuming the timing error $\epsilon T = 0.3$, we compare the MSEs of the FO-estimators (5) and (11) with their theoretical asymptotic variances. The results are depicted in Figures 1–2. Fig. 1 shows the results for a BPSK input constellation assuming a number of symbols $N = 50$. Fig. 2 shows the results for a QPSK input constellation with symbol number $N = 100$. It turns out that in the presence of ISI, the performance of FO-estimators (5) and (11) can be significantly improved by oversampling (fractionally-sampling) the output signal. This result is further illustrated by Figures 3–4.

Experiment 2-Performance w.r.t. timing error: In Figs. 3 and 4, the theoretical and experimental MSEs of the FO-estimators (5) and (11) are plotted versus the timing error ϵT, assuming the following parameters: SNR= 20 dB, $N = 50$ for BPSK constellation (Fig. 3) and $N = 100$ for QPSK constellation (Fig. 4). It turns out once again that oversampling of the received signal ($P = 4$) helps to improve the performance of estimators ($P = 1$) and to make the frequency offset estimators more robust to timing errors.

Experiment 3-Performance w.r.t. the number of input symbols N: The theoretical and experimental MSEs of the FO-estimators are plotted versus the number of input symbols N in Figs. 5 and 6 for BPSK and QPSK input symbol constellations, respectively, assuming the following parameters SNR= 20 dB and timing delay $\epsilon T = 0.3$. It can be seen that when the input symbol number N increases, the experimental results are well predicted by the theoretical bounds derived in Section IV. These plots also show that the proposed frequency estimators provides very good frequency estimates even when a reduced number of samples are used ($N = 20 \div 40$ samples). This shows the potential of these estimators for fast synchronization of burst transmissions.

Experiment 4-Taking into account all harmonics does not improve the performance of FO-estimators: Assume that the input symbol constellation is BPSK and $P = 4$. In this experiment, we want to compare the performance of estimator (5) with the one (7) which estimates f_e by taking into account all the three spectral lines of $\widetilde{C}_{2x}(\alpha;0)$. In Fig. 7, the solid line and solid line with stars denote the theoretical bounds of the estimators (7) and (5), respectively. Their experimental results are represented by dash line with circles and squares, respectively. Both theoretical and experimental results depicted in Fig. 7 show that estimator (7) does not improve significantly the performance of (5). In fact, the experimental mse-results of (7) are even worse than those of (5) in the lower SNR regime. This is due to the fact that the harmonics near the cycles of $\pm 1/P$ have small magnitudes and can be corrupted easily by the additive noise. Thus, taking into account all the harmonics is not justifiable from a computational and performance analysis viewpoint.

In a future paper, a complete analysis of these estimators will be presented together with extensions to other types of modulations (MSK, CDMA).

References

[1] J. C.-I. Chuang and N. R. Sollenberger, "Burst Coherent Demodulation with Combined Symbol Timing, Frequency Offset Estimation, and Diversity Selection," *IEEE Trans. Communications*, July 1991.

[2] P. Ciblat, P. Loubaton, E. Serpedin and G. B. Giannakis, "Performance analysis of blind carrier frequency Offset Estimators For Non-Circular Transmissions Through Frequency-Selective Channels," *IEEE Trans. Signal Processing*, Nov. 2000 (submitted).

[3] F. Classen, H. Meyr, and P. Sehier, "Maximum Likelihood Open Loop Carrier Synchronizer for Digital Radio," *ICC*, 1993.

[4] G. B. Giannakis and G. Zhou, "Harmonics in multiplicative and additive noise: parameter estimation using cyclic statistics," *IEEE Trans. Signal Processing*, Sept. 1995.

[5] F. Gini and G. B. Giannakis, "Frequency offset and symbol timing recovery in flat-fading channels: a cyclostationary approach," *IEEE Trans. Communications*, March 1998.

[6] E. Serpedin, A. Chevreuil, G. B. Giannakis and P. Loubaton, "Blind channel and carrier frequency offset estimation using periodic modulation precoders," *IEEE Trans. Signal Processing*, Aug. 2000.

[7] G. Zhou and G. B. Giannakis, "Harmonics in multiplicative and additive noise: performance analysis of cyclic estimators," *IEEE Trans. Signal Processing*, June 1995.

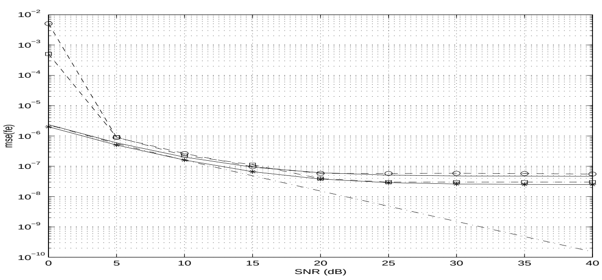

Fig. 1. MSEs of $\widehat{f_e T}$ versus SNR for BPSK constellation.

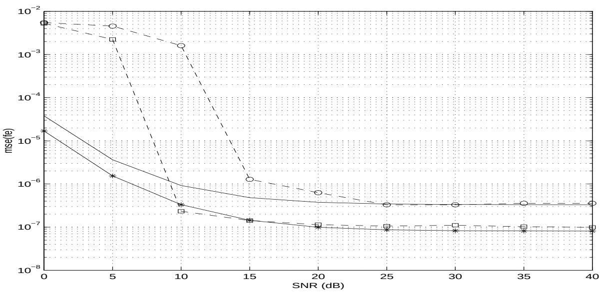

Fig. 2. MSEs of $\widehat{f_e T}$ versus SNR for QPSK constellation.

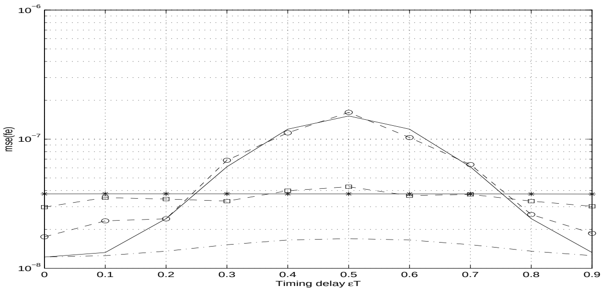

Fig. 3. MSEs of $\widehat{f_e T}$ versus timing error ϵT for BPSK constellation.

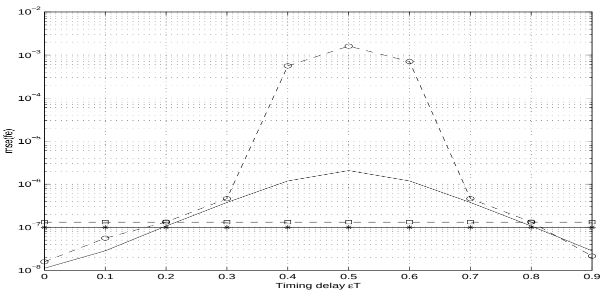

Fig. 4. MSEs of $\widehat{f_e T}$ versus timing error ϵT for QPSK constellation.

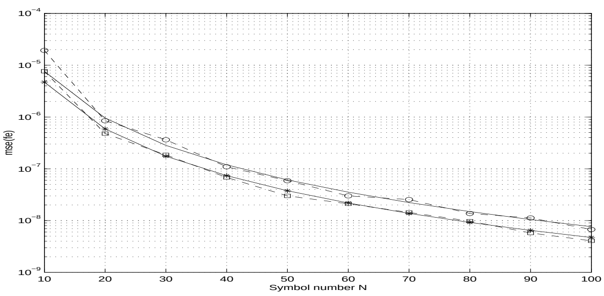

Fig. 5. MSEs of $\widehat{f_e T}$ versus symbol number N for BPSK constellation.

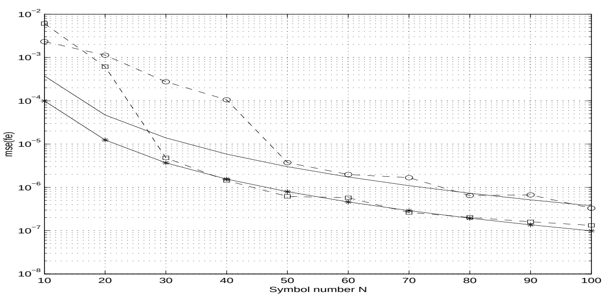

Fig. 6. MSEs of $\widehat{f_e T}$ versus symbol number N for QPSK constellation.

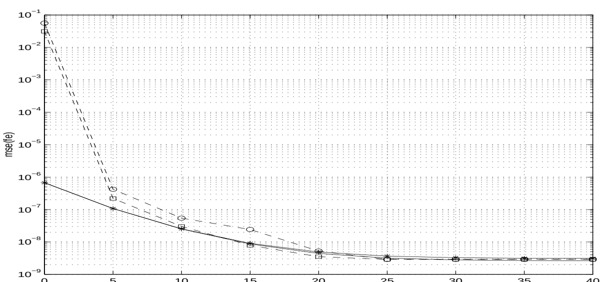

Fig. 7. MSEs of $\widehat{f_e T}$ of the estimators considering all harmonics and only one harmonic.